Challenging Glass 6 - Conference on Architectural and Structural Applications of Glass
Louter, Bos, Belis, Veer, Nijsse (Eds.), Delft University of Technology, May 2018.

ISBN 978-94-6366-044-0, https://doi.org/10.7480/cgc.6.2157

Dimensioning Silicone Joints Used in Bomb Blast Resistant Facade Systems

Pierre Descamps [a], Sebastien Durbecq [b], Valerie Hayez [a], Mahmoud Chabih [a], Georgette VanWassenhove
[a] *Dow Silicones Belgium, pierre.descamps@dow.com*
[b] *Internship from University of Louvain-La-Neuve, Belgium*

In the design of blast resistant glazing systems, gluing the laminate glass to the window frame with a structural adhesive is an attractive option to maintain it attached to the frame while, because the large deflection of the broken laminate, it could potentially escape from a mechanical fixing. Actually, it does not exist a simple method that provides guidelines to the facade maker to design a joint that will resist to a blast. The complexity to develop such a method is due to 1) the blast load is time dependent and the phase shift between the external load and the natural mode of vibration of the pane must be included in the model 2) modeling the deformation of a laminated glass after breakage of glass plies is complex. The intend of this study is not to propose the most accurate description of both the laminate and the joint deformation under a blast load but to identify which assumptions could be possibly made to simplify the problem and make possible the derivation of a simplified joint dimensioning method.

Keywords: Bomb blast; façade; silicone; joint; dimensioning

1. Introduction

After the Oklahoma City bombing in 1995 and one year after, the Canary Wharf bombing in London, bomb blast resistant facade became a more frequently demanded technical requirement for governmental buildings. A large number of fatalities was associated to people being hit by the glass shards or other debris coming from the blast or even more dangerous, the blow of all the laminate glass panel towards the inside of the building.

In the curtain wall industry, glazing systems are designed to keep a reasonable weight, also the facade is not primary designed to limit the damage in case of experiencing a blast but to protect the people occupying the building from the pressure wave and from all projections coming from the explosion. Sealant structural glazing has a big role to play in the design of bomb blast resistant facade systems. Indeed, when the laminated glass breaks, it loses its flexural rigidity and the pane deformation may become large enough to have the laminate escaping from its mechanical fixing. If dimensioned properly to prevent joint failure, a structural gluing of the laminate onto the frame is an attractive option to prevent this issue and maintain the laminate attached to the frame after glass plies breakage.

A recurrent demand comes from the curtain wall industry to develop a calculator to help them designing a structural joint that resists to a specified blast load. Building such a tool demands to identify which are the assumptions to be made to simplify the problem in a way that a joint calculation methodology can be developed that is simple enough to be transposable into an excel spreadsheet. Aligned with this objective, the goal of this study is not to propose the most accurate description of the behavior of a glazing system submitted to a blast but to understand which joint configuration is capable to maintain the broken laminate attached to the frame. We use FEA models of the full glazing system to understand which assumptions can be made to simplify the problem, those assumptions being highlighted in the text. First, we verify that we can reproduce the results published by Hooper et al [1] who simulates the glass laminate using 3 plies instead of 3 solid elements. After the breakage of the glass plies, Hooper set the elastic modulus of each glass ply to a very low value to simulate the reduced flexural rigidity of a broken laminate. We go one step further toward simplification in the simulation of the broken laminate using one single ply. Second, we demonstrate that the built-up of more complex models of a broken laminate requires the knowledge of parameters difficult to estimate like the percentage of delamination of the glass shards adhering to the interlayer. For this reason, using the elastic modulus of the PVB interlayer as a variable to adjust the model prediction to experimental data appears an acceptable option. Third, using a SDOF (single degree of freedom system), we show that we can calculate the deformation of the broken laminate at it maximum extension with good accuracy compared to FEA results Then, we connect the membrane to the joint via a free rotation point and calculate the joint deformation modeling the joint using springs. Finally, we study the sensitivity of the deformation of the structural joint with respect to the laminate deflection to determine with which degree of accuracy the laminate deflection have to be calculated.

2.Structural joint dimensioning to resist to blast load.

2.1. Glass pane deformation under dynamic load

To simulate the deformation of a glazing system experiencing a blast, the blast pressure evolution with time was modelled using the Friedlander waveform [2]. Alternative equations have been proposed that more accurately describes the negative phase of the pulse (for example, Rigby et al. [3]) but we select the Friedlander waveform because 1) it is broadly accepted by the facade industry and 2) the choice of the waveform will not impact the generality of this discussion neither the conclusions presented.

Hooper [1] has modelled a laminate using plates instead of 3D solid elements (laminate is simulated by 3 plies, two for the glass plates and one for the interlayer) and showed that before glass breakage, the two approaches leads to very similar results, this approach considerably decreasing the computation time. When the maximum principal stress in the glass plies reaches a threshold value of 80MPa, it is assumed that glass breakage occurs. Breakage is simulated by setting the Young's modulus of the glass plies to zero, not taking into account the impact of the glass shards adhering to the PVB interlayer on the flexural rigidity of the broken laminate. For this reason, the stiffness of the PVB interlayer has to be increased to fit the calculated bending amplitude of the laminate to the values observed experimentally.

In the Hooper approach, after glass breakage, the two glass plies have as sole role to have the correct mass for the laminated as it directly influences the dynamic behavior of the glazing system. For this reason, we made a further step toward simplification, modeling the broken laminate using a single ply, the total mass of the system being conserved by artificially adjusting the density of the PVB interlayer. The parameters used for FEA simulation are given in table 1. We will note that those parameters are rather atypical compared to what is done in the market, particularly the low glass thickness. They were selected to allow a direct comparison with the results published by Hooper. The comparison between the deflections using a one ply versus three plies model is shown in Fig. 1. The laminate deformation profile calculated using the two models at the time corresponding to the first peak in amplitude, (laminate deflecting towards the inside of the building) is shown in Fig. 2.

Table 1: parameters used for FEA modeling

FEA model parameters	Corresponding values
Larger glass dimension	1.5m
Smaller glass dimension	1.2m
PVB interlayer thickness	1.52mm
P_{max}	130kPa
t^+	6.5ms
Glass thickness	3mm

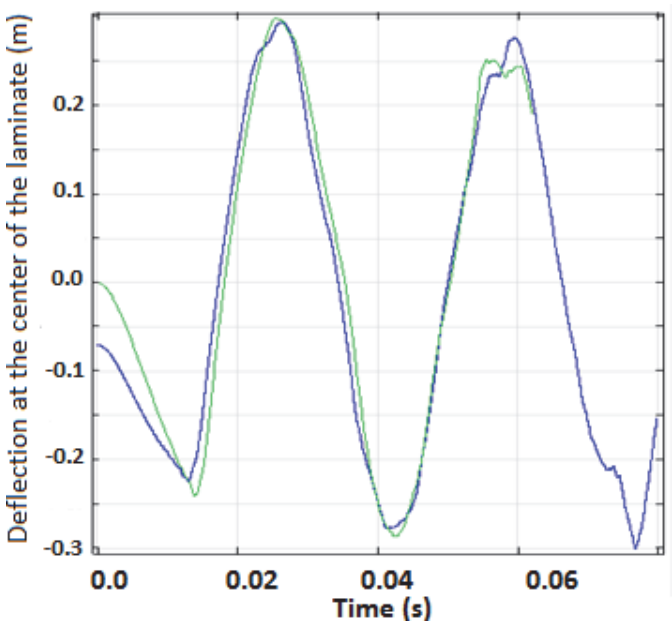

Fig. 1: comparison between the laminate deflection at its center calculated: 1) using a model with 3 plies having the glass modulus set to 10Mpa after glass breakage (blue curve) and 2) a model using one single ply model the broken laminate (green curve).

The Fig. 1 shows very similar results for the 2 models, the one ply approach allowing to gain one additional order of magnitude in computation time. Fig. 2 below shows the plate deflection profile calculated after a time of 14ms corresponding to the first peak in amplitude (deformation towards the inside of the building). We observe that the laminate deformation profile calculated using both models are very similar. For this reason, in the following of the study, this simplified one ply model will be selected.

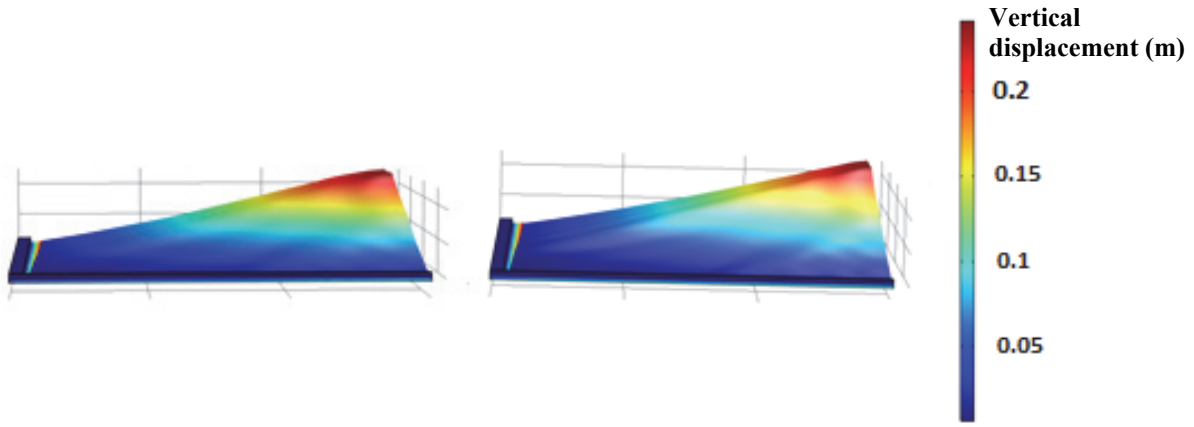

Fig. 2: Deformation profiles of broken laminate calculated using the 3 plies (left Fig.) and the 1 ply model (right Fig.) at a time corresponding to the first peak in deflection showing very similar results.

2.2. Why using the Hooper like approach; deformation of 2D laminates under static load

We may question the approach described by Hooper as it demands to adjust the stiffness of the interlayer to fit the experimental data. Indeed, it is known that the glass shards adhering to the interlayer increases the rigidity of the broken laminate. To illustrate this, a 2D model of a broken laminate was carried-out, each glass shards being modelled by a solid element adhering to the interlayer. Doing this model, we must assume that a certain fraction of the shards area has delaminated to insure convergence of the model. Indeed, the bending of the laminate imposes an extension of the interlayer connecting two adjacent shards. If shards are in direct contact, this displacement leads to an infinite local elongation of the interlayer and to a mathematical singularity. In addition, PVB manufacturer are not designing their material to prevent any delamination, as in this case, the high stress applying to the PVB interlayer at the junction of two shards would lead to PVB membrane breakage, which must be avoided. For this reason, assuming a fraction of shards having delaminated is a realistic assumption. Fig. 3a shows the deformation of the laminate at the junction between two shards located in the middle of the pane, the pane being submitted to a 100Pa static pressure. The color represents the spatial distribution of the first principal stress in the laminate; we observe that the higher stress values are localized in the junction with the shards but also at the border of the delamination zone. A deflection of ~ 1.0e-2 m is observed in the middle of the pane when assuming 33% of delamination. A similar deformation can be simulated using a single ply PVB interlayer but the PVD modulus must be increased by a factor 500.

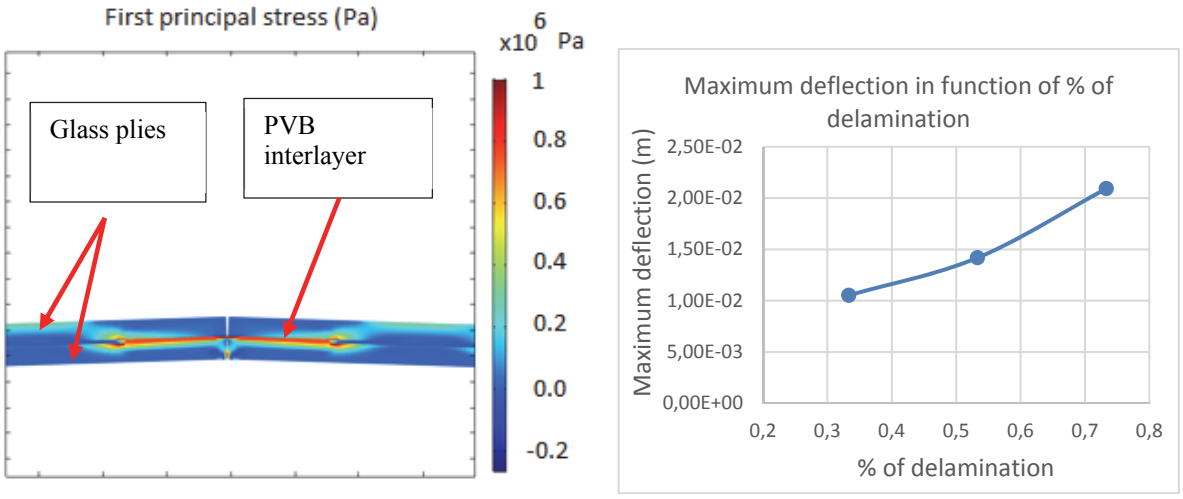

Fig. 3: a) distribution of first principal stress at the junction between two shards for 55% delamination b) maximum deflection of a pane in function of the percentage of PVB delamination.

The complexity of a model considering broken glass pieces results in the assumption that must be made about the percentage of the surface area of the shards having delaminated but also about the size and the shape of the broken glass pieces as it influences the bending rigidity of the broken laminate, those parameters being difficult to estimate and may vary, depending on PVB supplier for example. We have calculated the maximum deflection for 3 values of the percentage of delaminated surface (Fig. 3b). A significant impact of the % of delamination on the flexural rigidity of the laminate is observed.

The large of impact of the % of delamination of shards in the mechanical behavior of a broken laminated has been demonstrated by Galupi et al [4]; the author treats the case of a laminate submitted to equi bi-axial stress being applied in the plane of the laminate, and not transversally. The authors demonstrated than depending on percentage of delamination, the equivalent modulus of the laminate can vary by a factor 3.

Because of the uncertainty related to the model input variables and the long computation time associated to 3D modelling incompatible with industry demand, selecting an approach similar to the one proposed by Hooper makes a lot of sense. Of course, the fact that this choice is technically acceptable or not will depend on the impact that an error in the calculation of laminate deformation will have on the calculation of the stress distribution in the joint. This aspect will be treated below.

2.3. The dynamic deformation of glass laminate

In his paper, Hooper restricts his study to laminate deflection towards the inside of the building, stopping the time analysis at the maximum of the first deflection peak. In this time range, it is likely that the fundamental shape mode of excitation be dominant [5]. Using Hooper model, we calculated the glass pane deformation over a longer time period, covering the plate deformation when the plate is bending for and back (Fig. 5a-c). As 3mm thick glass plates are very unusual on the facade market (glasses abnormally thin), we decided in the following models to use 6mm thick glass plies which is closer to industry standards. The parameters used in the model to produce Fig. 5a-c are summarized in table 2 and an illustration of the pressure pulse given in Fig. 4.

Table 2: parameters used in FEA model (1 plie approach) to generate Fig. 5a-c

FEA model parameters	**Corresponding values**
P_{max}	100kPa
t^+	6.5ms
Larger plate dimension	2m
Smaller plate dimension	1.4m
Glass thickness	6mm
PVB thickness	2.25mm

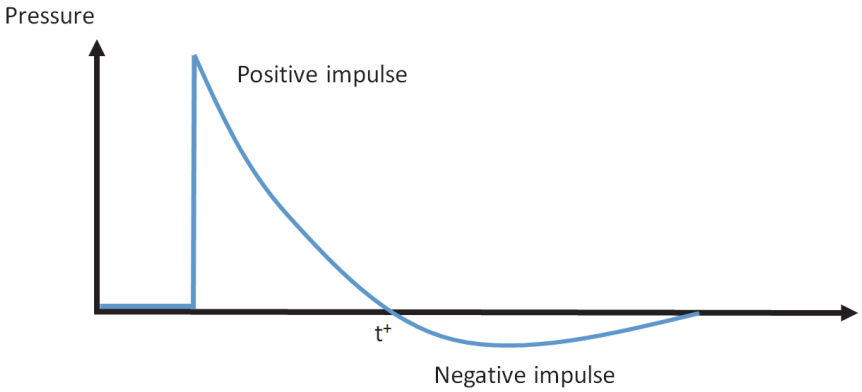

Fig. 4: illustration of the Friedlander waveform used to simulate a blast load.

Fig. 5a shows the spatial deformation of the laminate (deformation along the smaller side of the laminate) calculated 24 ms after the beginning of the explosion; the observed negative value of laminate deflection corresponds to a deflection towards the inside of the building. The time at which the deformation profile has been calculated is represented by a red vertical line on a graph representing the laminate deflection as a function of time. Laminate deformation calculated after a longer time delay (40ms and 50.5ms) are shown on Fig. 5b and Fig. 5c respectively.

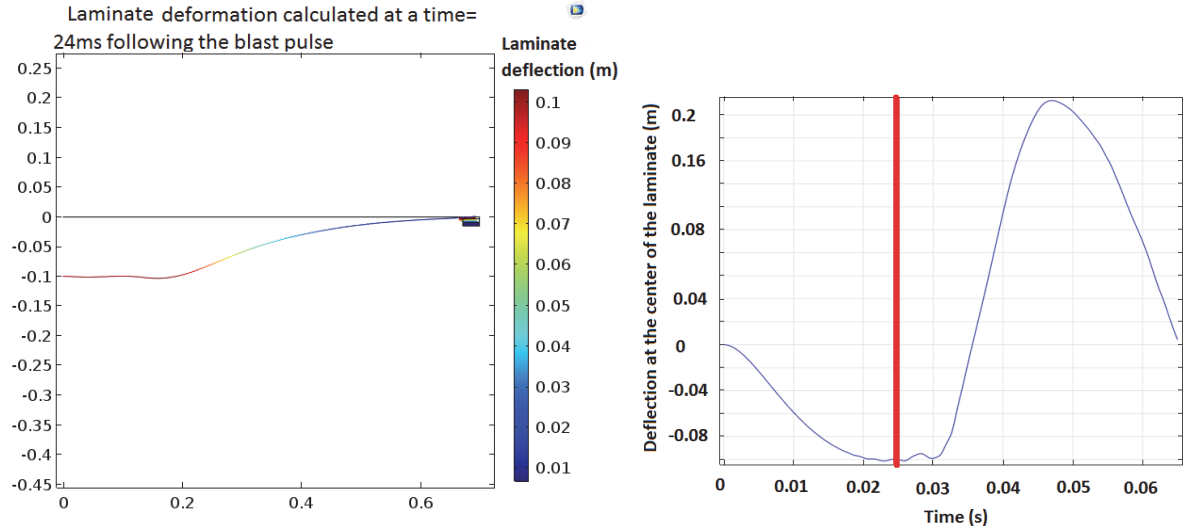

Fig. 5a: laminate deformation calculated at t=24ms (left Fig.); the red line on the right Fig. shows the deflection at laminate center corresponding to this time..

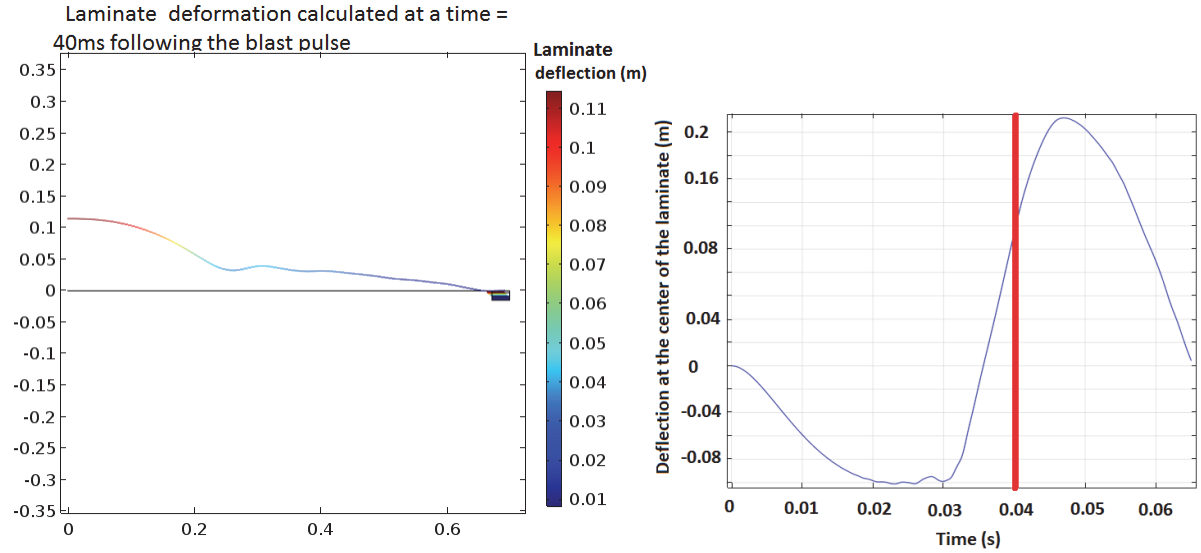

Fig. 5b: laminate deformation when moving towards the second peak of membrane deflection (t=40ms); pane bending is now directed towards the outside of the building.

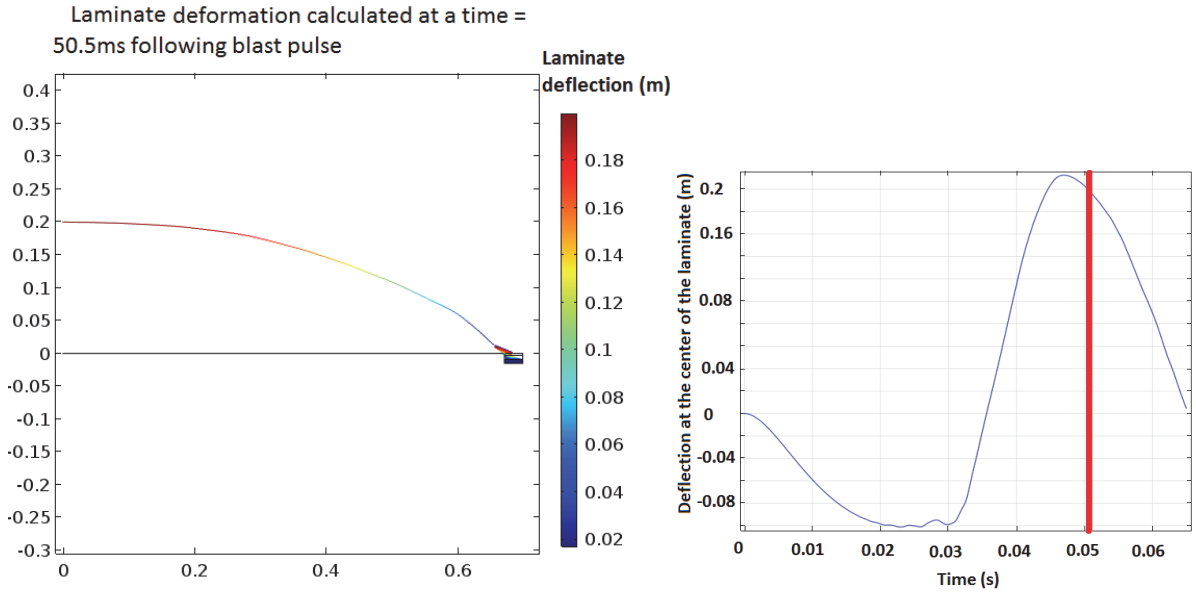

Fig. 5c: laminate deformation calculated at a time = 50.5ms following the beginning of the pulse. We observe a nearly parabolic deflection profile, with a maximum deflection amplitude of ~ 0.2m.

Because the mass of the system has increased (we increase the thickness of the glass ply), a different deflection pattern versus time is observed (amplitude and period) than the one shown on Fig. 1. We observe (Fig. 5a to 5c) that the deformation of the glass laminate deviates significantly from the fundamental bending mode, higher modes being excited by the blast. Higher modes excitation is explained by the following mechanism:

- During the positive pressure phase, the glass bends from the outside to the inside of the building, thanks to the positive pressure.
- After the positive pressure impulse, the glass pane continue to deform because of the inertia of the pane (and continues to bend towards the inside of building direction) even when the positive pressure pulse is finished ($t > t+$) and that pressure change sign.
- At the moment pressure changes sign (moving from positive pressure to suction when $t > t+$), the pressure opposes to the bending of the glass towards the positive direction.
- This phase shift between plate bending and suction force excites higher modes but also a reduction of the glass pane flexion as the external force is now opposite to displacement.
- Because there is little energy loss associated to glass deformation, most of the energy associated to glass deformation is recovered and glass pane keeps its oscillation like a spring system.
- Glass bending towards the outside of the building is now in phase with the suction force, leading to enlarged deformation at the second flexion peak. This mechanism explains why, in most of bomb blast test, the glass being detached from the frame is in front of the façade because it is during the second deflection peak that glass pane deformation and stress in the joint are the largest.

The interference between the plate continuing to bend on its inertia and the suction force in opposite direction creates complex deformation pattern of the laminate particularly visible in the transition period between the two first peaks of deflection at the center of the laminate (the 2 peaks corresponds to deflections in opposite directions). But the maximum deflection at the vicinity of the second peak has a deformation profile very close to a parabolic shape (Fig. 5c). We do not want to predict when the glass laminate will break but study the ability of the structural joint to maintain the laminate attached to the frame after glass plies breakage. We will assume that the glass will break and study how far the stress in the joint increases because of increased laminated flexibility. For this reason, we will not focus our study on the calculation of the stress pattern in the glass plies during the transition period between the two first peaks of deflection of the center of the laminate.

The maximum value of the joint deformation and related to it, the maximum value of the first principle stress are shown on Fig. 6.

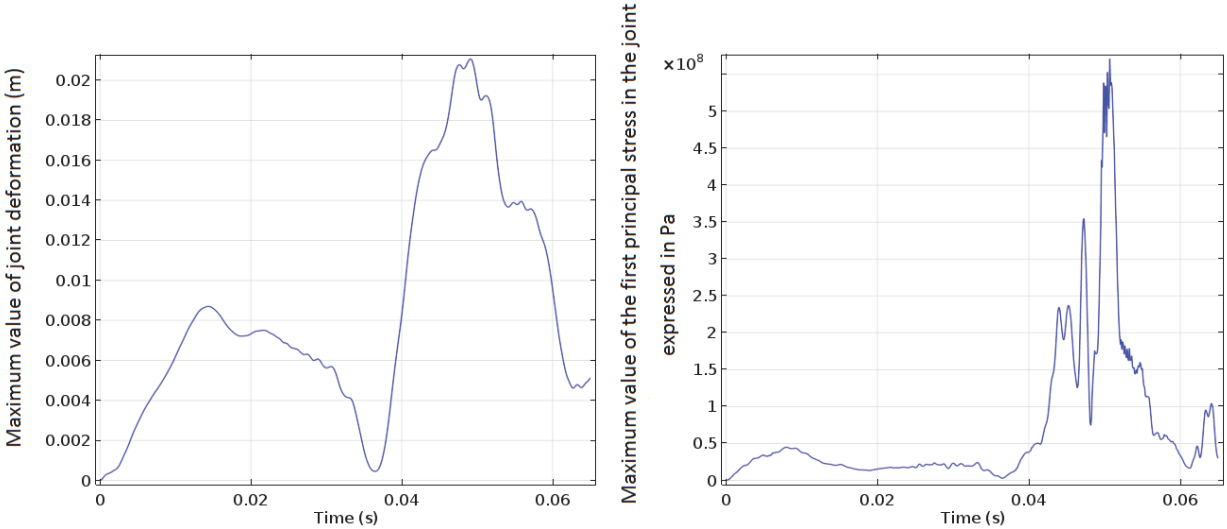

Fig. 6: Time evolution of the maximum values of: a) joint displacement (and so elongation) and (b) First principal stress. The values are calculated in a joint cross-section located in the middle of the longer side of the laminate.

We observe a large maximum of deformation (and a maximum in first principal stress) that corresponds to the laminate deformation represented in Fig. 5c, the plate showing a deformation close to a parabolic profile corresponding to a membrane in tension. This deformation profile is similar to the deflection of a glass pane submitted to a static load when the plate deformation is >>> compared to plate thickness. We are in those conditions as the laminate displacement observed during bomb blast experiments after glass breakage can be as large as 0.2m. An analytical solution to calculate the nonlinear large deformation of thin rectangular plate submitted to a static load is a complex problem and multiple solutions have been proposed in the literature [6, 7, 8]. In his Phd thesis [6], Berger proposes an approximate formula to calculate large deflection of a thin plate under static load; the glass deflection calculated using

Berger's solution stands in between the solution proposed by Levy [7] (Levy assumes simply supported boundary conditions with free edges lateral movement) and the solution proposed by Wang [8] (who assumes zero lateral edge movement). Knowing that silicone joint will somehow limit the pane displacement/deformation at his edge, the "in between" nature of Berger solution appears very appropriated for our case.

Glass pane deformation W proposed by Berger is given by:

$$W = h\left(\frac{q\,a^4}{D\,h}\right)^{1/3}\left(\frac{\frac{1}{2}\left[1-\left(\frac{x}{a}\right)^2\right]-\sum_{n=0}^{\infty}\frac{2(-1)^n\cosh(\beta_n y)\cos(\beta_n x)}{(\beta_n a)^5\cosh(\beta_n b)}}{\left(2-12\frac{a}{b}\sum_{n=0}^{\infty}\frac{\tanh(\beta_n b)}{(\beta_n a^5)}\right)^{1/3}}\right) \quad (1)$$

Where h is the glass pane thickness, a and b are half the value of the smallest and largest pane dimensions, q is the pressure load, D is the flexural rigidity and $\beta_n = \frac{2n+1}{2\,a}\,\pi$

The glass pane deflection predicted by the Berger formula under a static load has been compared to the deformation calculated at a time t=50.5 ms using FEA (Fig. 7) that corresponds to the second maximum deflection peak. We observed that Hooper model predicts a deformation equal to the deformation of a thin plate (membrane) under static load, a deformation probably close to reality.

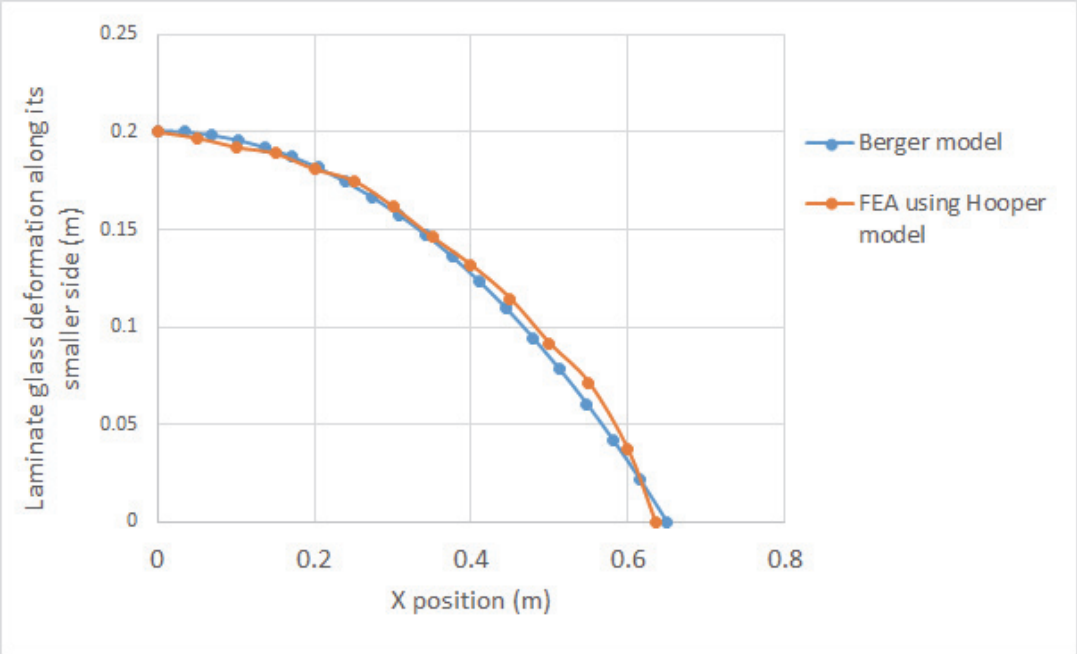

Fig. 7: comparison between the deformations along the small glass side calculated at the moment of the second peak of maximum deformation using the Hooper FEA model and the Berger relation (thin plate defection under static load).

2.4. Modelling the pane deformation by a one degree of freedom system

In structural engineering, the dynamic behavior of a structure is often modelled using a single degree of freedom system [9]. This phenomenological analogy allows to reduce the problem to a one variable ODE that can be either resolved analytically or using a simple 1D integration routine. The blast-resistant community considers that such SDOF idealization is an acceptable representation of a blast –resistant glazing system because the plate response is assumed to the dominated by the first mode [10,11,12]. This model consists of a spring having a stiffness constant k and a mass corresponding to the mass of the system (Fig. 8). Because the glass pane deflection is non-linear, we note that the spring stiffness coefficient is a function of the displacement y.

Fig. 8: simplified analogy between a mass spring system and a plate deformation under external load

The equation of such system can be written:

$$M\,\ddot{y} + k(y)\;\; y = F(\mathrm{t}) \tag{2}$$

Where m is the mass of the system, k is the spring stiffness being a function of spring elongation and F, the external force applied. This force can be the Friedlander waveform defined before.

There are two difficulties when building a SDOF model. First, we must find a spring stiffness coefficient that predicts accurately the large deflection of a thin plate under a large static load. At this stage, we propose to use the Berger formula defined before. Second, when carrying out a SDOF model, the total system mass and load must be replaced by equivalent values to include the fact that not all points of the laminate experience a unique displacement value. The equivalent load is calculated assuming that the total work done by the load on the plate and the work done by the load on the SDOF masse are the same.

The work done by the load in the real system is:

$$F_e = \int q\;\; \varphi(x,z)\;\; dx\, dz \tag{3}$$

With q is the pressure and φ the shape function of the plate that represents the spatial plate deformation in the y direction normalized by the maximum deflection at the plate center (to have φ dimensionless as required by (3)). In our case, we select φ being equal to the normalized Berger function (eq. 1).

The load factor F_M is calculated as:

$$F_M = F_e/F_t$$

Where F_t is the total force applied to the system equal the pressure multiplied by the surface.

Similarly, an equivalent mass M_e of the SDOF system is calculated by:

$$M_e = \int m_a\;\; \varphi(x,y)^2\; dx\, dy \tag{4}$$

Where φ is the shape function as defined before and m_a the mass per unit surface of the plate.

The mass factor K_M is defined as:

$$K_M = M_e/M_t$$

Where M_t is the total mass of the system equal to masse per unit of the laminate plate multiplied by the plate surface area.

The equation of SDOF system is equivalent to real system when multiplying the mass by the K_{LM} factor, being the ratio between K_M and K_L. Carrying-out both integration, we obtain a load mass factor of 0.67 for a plate of aspect equal to 1.4. This value is close to the one use in the HAZL codes [13] that proposes a load mass factor dependence on plate aspect ratio equal to:

$$K_{LM} = 0.63 + 0.16\;(\mathrm{AR}\;\; -1) \tag{5}$$

Where plate aspect ratio AR is defined as the ratio between the larger and the smaller pane dimension.

The SDOF equation is integrated to calculate the evolution of the maximum glass pane deflection in function of time. We have used the same process parameters than for the FEA calculation (Table II) to allow a direct comparison between the SDOF model and of the FEA model (Fig. 9). We observe that both two first peaks are located at the same time for both models. In addition, the amplitudes of the first peak are very close. A smaller amplitude of second peak is obtained solving the SDOF equation which can have two explanations: 1) the Berger solution (equation 1) does not accurately describe the nonlinear deformation of the laminate 2) we cannot assume like in the SDOF model that plate deformation is mainly driven by the fundamental mode. As we observe a good fit between the models for the first peak (dominated by the fundamental mode), we can conclude that the nonlinear behavior of the plate deformation is well described by the Berger solution. The difference observed for the second peak is thus most likely associated to higher modes excitation, as it was illustrated by Fig. 5-b.

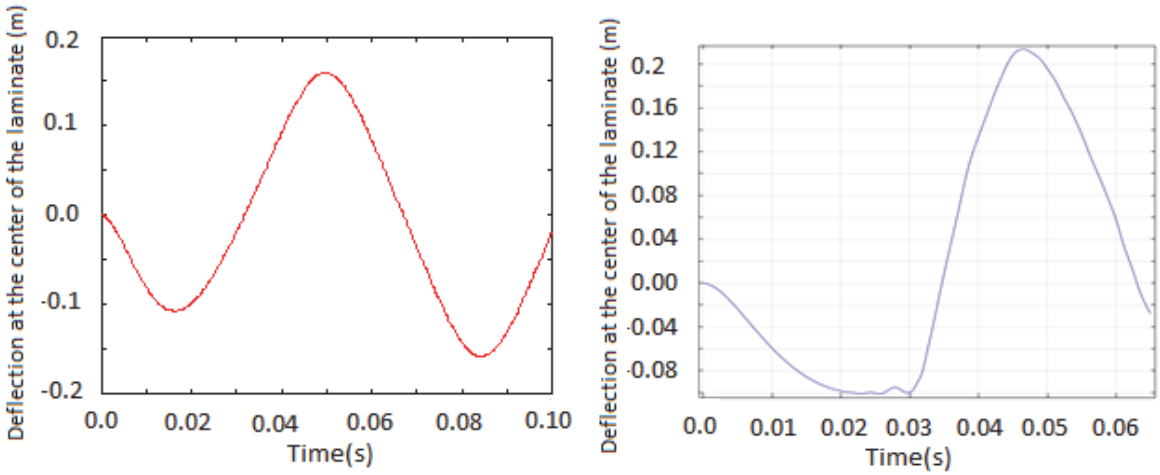

Fig. 9: Calculation of the membrane deformation resolving SDOF system equation or using FEA model with a single ply.

Using Berger solution to describe spring stiffness in the SDOF model, we implicitly assume that the deflection profile of the broken laminate is not significantly influenced by the joint geometry. To verify this assumption, we carried-out a 3D FEA models, changing the geometry of the joint. The joint geometries tested are summarized in table 3 and the model outcome is presented in Fig. (10).

Table 3: Calculation of membrane deflection, variation the geometry of the structural joint attaching the laminate to the frame

Joint bite	Joint Thickness	Joint aspect ratio= bite / thickness
28 mm	6 mm	4.7
16 mm	6 mm	2.7
28 mm	12 mm	2.33
16 mm	12 mm	1.33

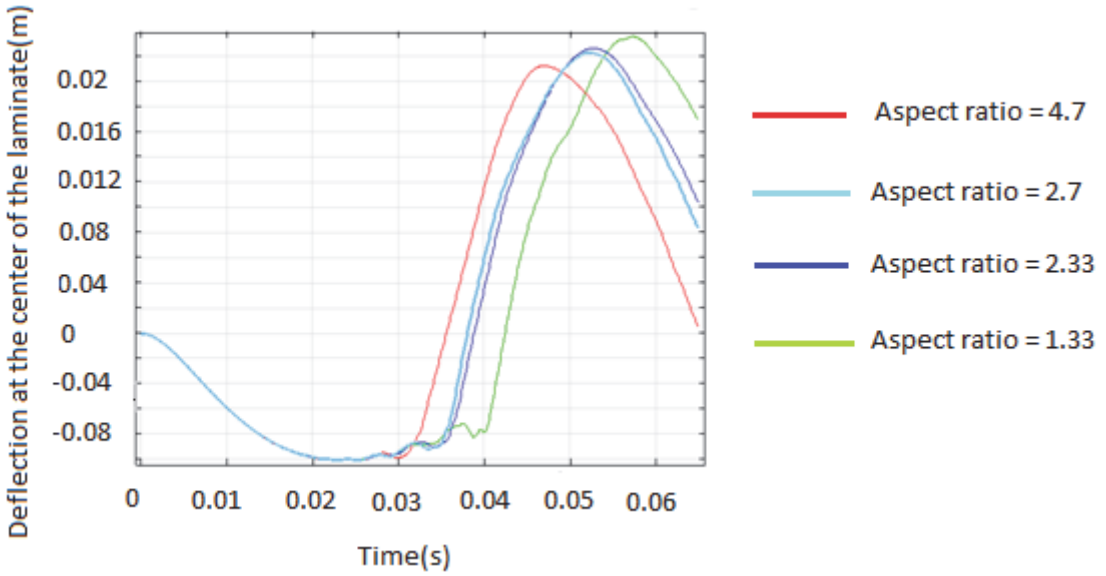

Fig. 10: Time dependence of the maximum deformation of a broken laminate in function of time, the pane being fixed by structural joints having different shape and dimensions.

The impact of joint aspect ratio the rigidity of a joint has been demonstrated in a previous work and published in [14]; amongst the tested geometries, the 28*6 mm^2 joint possesses the greater rigidity (larger bite, low thickness, large aspect ratio). Joint rigidity influences the membrane deflection as the amplitude of second peak is smaller and the maximum deformation occurs earlier than for other joint geometries.

This result is expected, knowing that the natural period of vibration of a SDOF system is:

$$\omega = \frac{2\pi}{T} = \sqrt{\frac{K}{M}} \tag{6}$$

With K, the constant of rigidity of the spring and M the mass. When the joint rigidity increases, the natural frequency of vibration of the system increases and so the period of oscillation is decreased.

The green color represents the more flexible joint, the amplitude of deformation being the larger and peak maximum being delayed compared to other geometries. The pale and marine blue colors show very close behavior even if joint dimensions are different but they have very close values of aspect ratio. We can refer again to the paper publish in CGC5 [8] where it was showed that joint rigidity is mainly dependent on the joint aspect ratio. Even if joint influences membrane deflection, the effect is not that large and it is very possible that those differences will have a minor effect on calculated joint deformation. This point will be examined at the end of the next paragraph.

2.5Modelling Stress transfer to the joint

Knowing the vector force that applies to the point of attachment of the laminate to the joint, 3 models can be made to describe the connection point (Fig. 11);

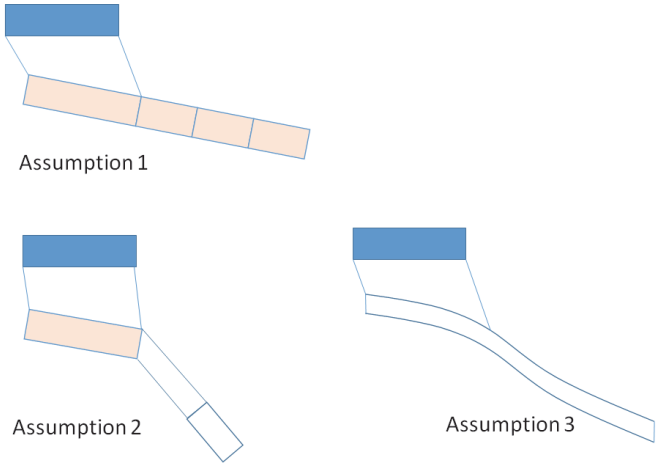

Fig. 11: Representation of the possible assumption that can be made about the attachment of broken laminate to the joint.

The first case is not relevant because it assumes that the flexural rigidity of the broken laminate is much greater than joint rigidity, which is the case before glass plies breakage but not after. The second case assumes a change of slope of laminate deflection at joint extremity, having a free rotation connection at this point. The third case assumes that the membrane stays soft, even at joint location. The case 2 seems the more realistic because the laminate should be more rigid at joint location because either the glass did not break there or the joint locally rigidify the broken laminate. A larger laminate bending at the extremity of the joint also creates a large local stress between the glass shards and the PVB interlayer, making the shards detaching from the laminate. The absence of shards will make this point even more flexible, justifying the free rotation connection assumption (this assumption is critical to simplify the model and even being in accordance with intuition, it must be validated by the experiment). The joint deformation problem can now be treated as illustrated in Fig. 12.

To model the joint, we will use the approach presented in CGC5 [14] where the joint was modeled by springs. However, using spring, we do not impose the volume conservation of the joint, which is critical. Indeed, the interface of adhesion to the substrate cannot reduce, and because silicone is nearly incompressible, it induces a high local stress at the interface with the substrate. Feyman shows that this effect influence the rigidity modulus of the joint which can be significantly larger than the Young modulus [15]. We demonstrate that this effect can be described by a joint rigidity factor that only depends on the joint aspect ratio. Using this rigidity factor to the joint submitted to tension to calculate the spring stiffness, we somehow “inject” the joint volume conservation into a spring model.

In the CGC5 paper, we assumed that the glass pane is much more rigid than joint and impose a rotation to the joint. For this reason, to calculate joint deformation, only force balance equations are required as the angle of rotation is assumed to be known (calculated using simply supported glass plate assumption). In the case illustrated in Fig. (12), as the angle of rotation α is unknown, one more equation must be added to close the system, resolving both force and momentum balance equations.

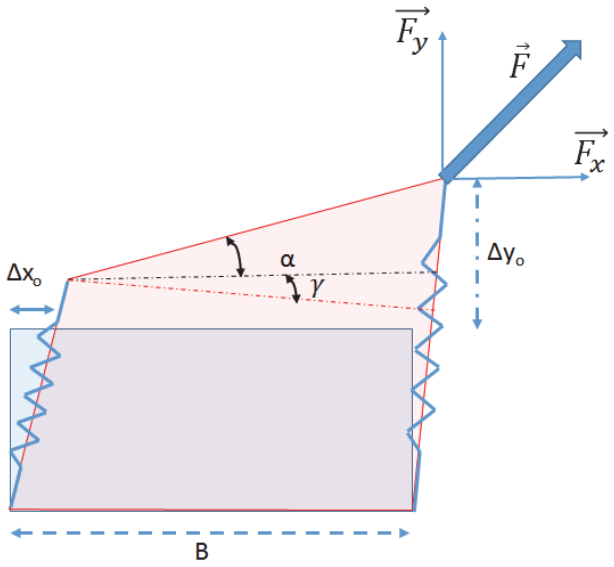

Fig. 12: Joint modelled using two springs, a force being externally applied to a free rotation point located at the upper right corner of the joint.

If we assume the joint described by 2 springs (Fig. 12) and that we consider small rotation angle values, the force balance can be written:

$$F_x = G\,\frac{B}{e}\,\Delta x_0 \tag{7}$$

$$F_y = E\,\frac{B}{e}\,\Delta y_0 + E\,\frac{B^2}{2\,e}\,\sin(\alpha) \tag{8}$$

Where F_x and F_y are the x and y component of the force applied to the free rotation point, B is the joint bite, e the joint thickness, E and G are the springs stiffness in tension and shear, Δx_0 and Δy_0 the lateral and the transversal joint displacement and α, the angle of rotation.

The momentum balance gives:

$$F_x B sin(\alpha) - F_y B\, sin(\alpha) = \frac{B^2\,E}{2\,e}\,\Delta y_0 \cos(\alpha+\gamma) + \frac{B^3\,E}{2\,e}\sin(\alpha)\,\cos(\alpha+\gamma) \tag{9}$$

If we assume a small joint rotation, we have cos $(\alpha+\gamma)\sim 1$ and sin $(\alpha)\sim\alpha$

$$F_x\alpha - F_y\alpha = \frac{B\,E}{2\,e}\,\Delta y_0 + \frac{B^2\,E}{2\,e}\,\alpha \tag{10}$$

In above equations, E is the stiffness constant of the spring working in tension. E is equal to the material Young's modulus multiplied by the rigidity factor to take into account volume conservation under traction. As no volume change is associated to pure shear, the shear modulus G is taken equal to $\frac{Eyoung}{2(1+\nu)}$ where ν is the Poisson's ratio. As a silicone material is nearly incompressible, we can assume $\nu\sim 0.5$ to have $\sim \frac{Eyoung}{3}$.

The accuracy in the momentum calculation depends on discretization and on the number of springs used to model the joint. Extending the calculation for a number of springs $n \to \infty$, we find:

$$\sin(\alpha) = \frac{\frac{3\,F_y}{2}}{F_x + \frac{E\,B^2}{e}\left(\frac{1}{4} - S\right)} \tag{11}$$

$$\Delta y_0 = \frac{F_y - \frac{E\,B^2\sin(\alpha)}{2\,e}}{\frac{E\,B}{e}} \tag{12}$$

$$\Delta x_0 = \frac{F_x\,e}{B\,G} \tag{13}$$

With S, a series that depends on the number of springs used for calculations; you can verify that at least 6 springs are needed to accurately calculate the momentum:

$$S = \frac{1}{n} \sum_{i=1,n-1} \left(\frac{i}{n-1}\right)$$

We have compared the results of this simplified model to the calculation carried-out by finite element analysis. The geometry and material parameters used for the calculations are summarized in table 4. The rigidity factor law in function of the aspect ratio we used has been one published in [14].

Table 4: Parameters use of the modeling of a silicone joint having a force applied to a free rotation point located at the upper right part of the joint.

Model parameter (FEA and spring model)	Corresponding values
B (joint bite)	30 mm
e (joint thickness)	12 mm
Applied Force (N/m)	1e4 N/m
Angle of the force applying to the free rotation point with respect to the horizontal line	π/4
E_{Young}	2.1e6 MPa

The joint deformation calculated by FEA and using the spring simplified model are compared on Fig. (13) and the maximum joint displacement along x and y axis are summarized in table 5.

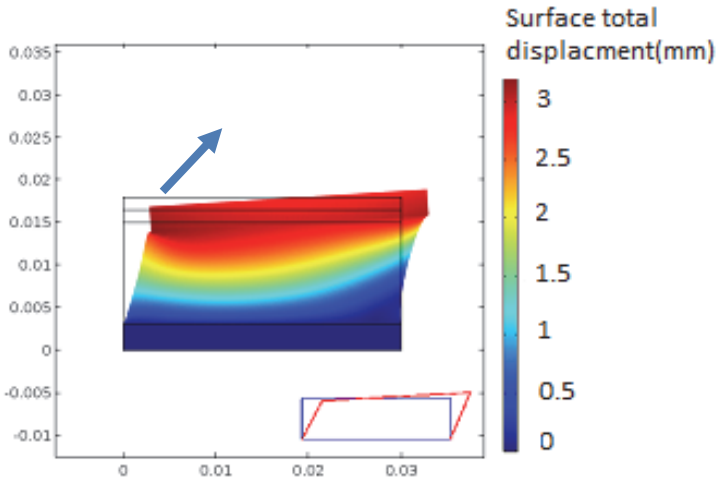

Fig. 13: joint deformation under a force of 1e4 N/m applied on a free rotation point; comparison between FEA and spring model.

Table 5: comparison between lateral and transversal joint displacement calculated by FEA or using the spring model

Type of Model	Δ x (displacement along x)	Δ y(displacement along y)
FEA model	3.98 mm	1.78 mm
Spring model	4 mm	1.7 mm

We observe a good agreement between FEA calculation and the spring model. This means that the rigidity factor law in function of aspect ratio describes correctly the joint rigidity change with its geometry. Using the simplified spring model, we study the sensitivity of the joint deformation to a variation of the orientation of the vector force applying to the free rotation connection point of the laminate to the joint. The maximum value of local joint displacement $\sqrt{\Delta x^2 + \Delta y^2}$ is calculated in function of the angle α (angle of external force to the joint) for a force of 1e4 N/m applied to the joint (Fig. 14).

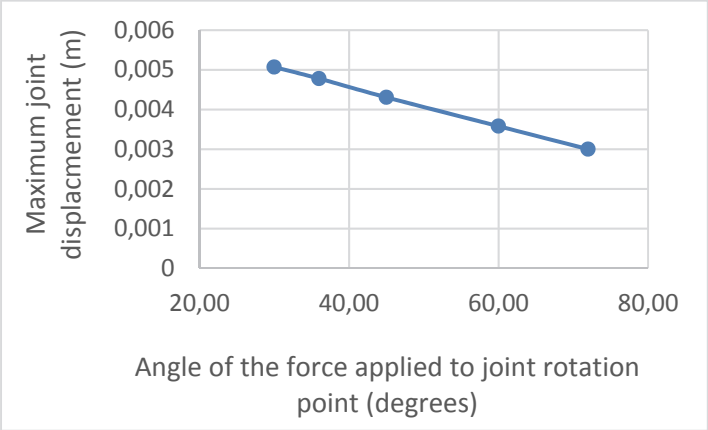

Fig. 14: Maximum value of local displacement of a joint submitted to a force of 1e4 N/m applied with different angle at a free rotation point located to the upper right part of the joint.

We observe that total joint deformation is not too sensitive to the vector force orientation, which is a consequence of the assumption of a free rotation connecting point. An error of 20 degree in the angle calculation leads to an error on maximum joint deformation comprised between 20 and 25%, depending in the value of the angle. This means that it is not necessary to build to very complex models of laminate deformation if we are only interested in the joint deformation and its capability to maintain the laminate in place after breakage. If making sense, this assumption of free rotation connection of the membrane to the joint is critical for the above conclusions and must be validated by experimental observations.

2.6. Importance of a formula that integrates joint thickness

An important aspect of the simplified model to calculate the joint deformation is that it includes both joint bite and thickness but also the material elasticity, via the Young's modulus, all these parameters being degrees of freedom available to design the joint that will not fail under the blast.

The importance of joint thickness is illustrated in Fig. (15) where we calculate the Von Mises stress spatial distribution in the joint for 2 different joint thicknesses of 15 mm and 8mm. The laminate characteristics are the ones given in table II. We observe a very similar spatial stress distribution for the two different joint configurations but the absolute values of the stress are very different (different selected color scales). The maximum value of VM stress (orange color) is ~ 5e6 Pa for the 15mm thick joint and 10e6 Pa for the 8mm thick joint.

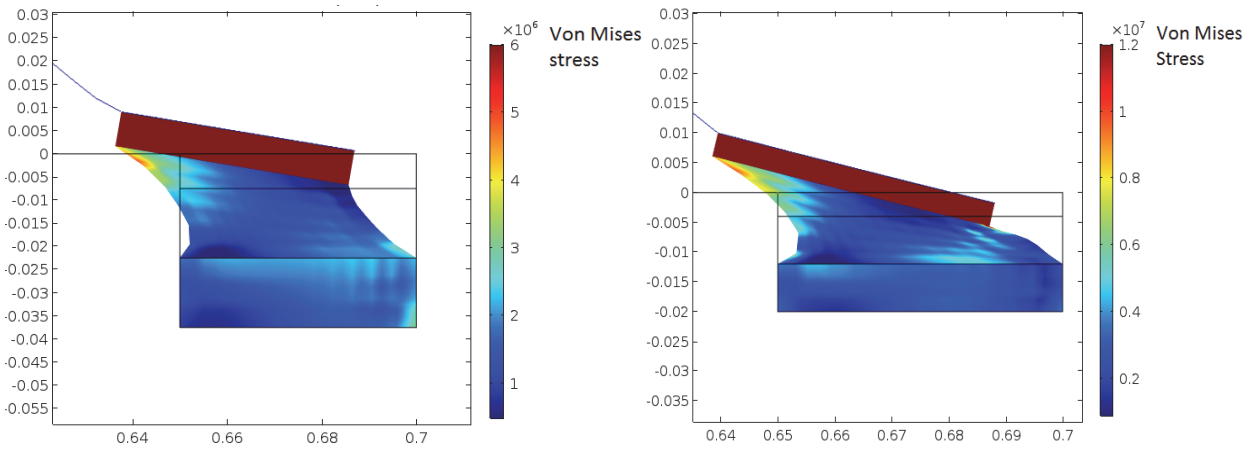

Fig. 15: Von Mises stress distribution in a joint of same bite of 50mm and a joint thickness of respectively a) 15 mm and b) 8mm.

We also carried-out glazing system modeling for a joint 8mm thick but considering a Young's modulus divided by 2 (Fig. 16).

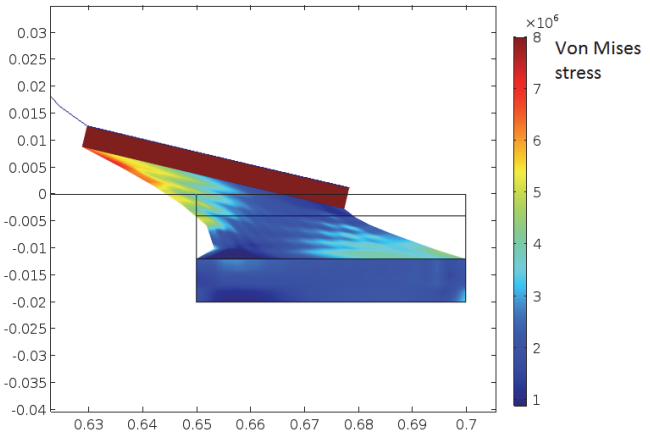

Fig. 16: Joint geometry corresponding to Fig. 12b but with sealant Young's modulus divided by a factor 2.

The maximum Von Mises stress value in a joint of lower Young's modulus is equal to 6.7Mpa (orange color) compared to 10MPa, representing a VM stress reduction of more than 30%. We insist at this point that using a material of lower Young's modulus is only beneficial if Young's modulus decrease is not detrimental to the tensile strength value: a sealant should have a lower modulus but keeping at least a same tensile strength, and so having a larger elongation at break.

3. Conclusions

Different models were built to understand the behavior of a glazing system under blast loading and identify where assumptions could be made to simplify the problem of structural joint dimensioning (geometry and properties of joints)

Building a realistic model of a broken laminate is very complex and time consuming, and cannot be made for each building specificities. In addition, we showed that such model demands the knowledge of model inputs difficult to measure like the degree of delamination of the glass shards or the shape distribution of broken elements. A decent description of broken laminate behavior can be obtained using a single ply approach with the PVB elastic modulus being increased, the elastic modulus being a variable to adjust the model to experimental data. A good description of the dynamic of laminate is observed combining a SDOF approach with an appropriate nonlinear model of a pane deformation to define the spring stiffness. Doing so, the force vector applying to the joint can be estimated with sufficient accuracy.

Assuming that the connection of the laminate to the joint is a free rotation point (an assumption that must be validated) we were able to calculate the joint deformation using a spring model, incorporating material volume conservation in the equation via a joint rigidity factor, the model giving good agreement with FEA modelling. With the free rotation assumption, we showed that joint deformation is lowly depending on the angle of the force applying to the rotation point, showing that this angle does not need to be determined with too much accuracy.

The approach proposed allows to understand joint deformation or maximum stress, considering both the joint geometry (joint bite, thickness and aspect ratio) but also of material mechanical properties. This is critical as the joint thickness and material modulus have a key impact in the joint capability to sustain the constraints generated by the blast.

References

[1] Hooper et al, International Journal of solids and structures 49 (2012) – pp 899-918.
[2] Dewey J. M. 'The shape of the blast wave: studies of the Friedlander equation', 21st International Symposium on Military Aspects of Blast and Shock, Israel 2010
[3] Rigby S. E.et al., 'The negative phase of the blast load', International Journal of Protective Structures, vol. 5, N 1, March 2014.
[4] Laura Galuppi, G. Royer Carfagni, Composites part B, 111 (2017)- pp 332-347.
[5] Abraham Menzin, 'Innovative Topics in Structural Engineering and Real Estate Development:
Blast Resistant Facades & Incentives for Large-Scale Smart Growth development', Master Thesis, Massachusetts Institute of Technology, June 2006.
[6] Berger H., 'A new approach to the analysis of large deflection plates', Phd Thesis, California Institute of Technology (Caltech), 1954.
[7] Levy S., 'Bending of rectangular Plates with large deflections', NACA TR 747, 1942.
[8] Wang, Chi-Teh, 'Bending of rectangular Plates with large deflections', NACA TR 1462, 1948
[9] J. M. Biggs, Structural dynamics, McGraw-Hill book company, New York, San Francisco, Toronto, London, 1964.
[10] T. Ngo et al, 'Blast loading and blast effects on Structures – An overview', EJSE Special Issue Loading on Structures (2007).
[11]A. T. Hussein, 'Non-0linear Analysis of SDOF System under Blast Load', European Journal of Scientific Research, Vol 45, N.3, (2010), pp. 430-437.

[12]J. C. Gannon et al, ' Approximation of blast loading and single degree-of-freedom modelling parameters for long span girders', WIT transactions on State of the Art in Science and Engineering, Vol 60, (2012)pp153-162.
[13] HAZL, Protective Design Center, Omaha District Corps of engineers, NE, 1998.
[14] P. Descamps V. Hayez, M. Chabih, 'Next generation calculation method for structural silicone joint dimensioning', CGC5, 2016 – also published in: Glass Struct. Eng. June 2017.
[15] Feynman, R., Leighton, R.M., Sands, M.: Lectures on physics, Vol. II, Copyright 1963, 2006, 2010 by California Institute of Technology, Michael A. Gottlieb, and Rudolf Pfeiffer (1963).